



Investigation of the feasibility for 3D synthetic aperture imaging

Nikolov, Svetoslav; Jensen, Jørgen Arendt

Published in:
Proceedings of 2003 IEEE Symposium on Ultrasonics

Link to article, DOI:
[10.1109/ULTSYM.2003.1293287](https://doi.org/10.1109/ULTSYM.2003.1293287)

Publication date:
2003

Document Version
Publisher's PDF, also known as Version of record

[Link back to DTU Orbit](#)

Citation (APA):
Nikolov, S., & Jensen, J. A. (2003). Investigation of the feasibility for 3D synthetic aperture imaging. In *Proceedings of 2003 IEEE Symposium on Ultrasonics* (Vol. 2, pp. 1903-1906). IEEE.
<https://doi.org/10.1109/ULTSYM.2003.1293287>

General rights

Copyright and moral rights for the publications made accessible in the public portal are retained by the authors and/or other copyright owners and it is a condition of accessing publications that users recognise and abide by the legal requirements associated with these rights.

- Users may download and print one copy of any publication from the public portal for the purpose of private study or research.
- You may not further distribute the material or use it for any profit-making activity or commercial gain
- You may freely distribute the URL identifying the publication in the public portal

If you believe that this document breaches copyright please contact us providing details, and we will remove access to the work immediately and investigate your claim.

INVESTIGATION OF THE FEASIBILITY OF 3D SYNTHETIC APERTURE IMAGING

Svetoslav Ivanov Nikolov and Jørgen Arendt Jensen

Center for Fast Ultrasound Imaging, Bldg 348, Ørsted•DTU, Technical University of Denmark
DK-2800 Lyngby, Denmark

Abstract - This paper investigates the feasibility of implementing real-time synthetic aperture 3D imaging on the experimental system developed at the Center for Fast Ultrasound Imaging using a 2D transducer array. The target array is a fully populated 32×32 3 MHz array with a half wavelength pitch. The elements of the array are grouped in blocks of 16×8 , which can simultaneously be accessed by the 128 channels of the scanner. Using 8-to-1 high-voltage analog multiplexors, any group of 16×8 elements can be accessed.

Simulations are done using Field II using parameters from a 32×32 elements experimental array made by Vermon with a center frequency of 2.93 MHz, fractional bandwidth of 58 %, and a pitch of $300 \mu\text{m}$. The simulations show, that using all of the 128 elements a spherical wave within ± 50 degrees sector can be created. The level of the edge waves is reduced by applying apodization with an elliptic footprint.

The results of simulations show that the angular resolution at -6dB is 2.7 degrees, and is determined by the distance between the outer-most transmit elements. The peak grating-lobe levels are -23.5, -25, 27.2, -44.5 dB below the main peak for 64, 100, 144, and 169 transmit events, respectively. The number of scanned volumes per second for these cases are 78, 50, 34 and 30, respectively.

I INTRODUCTION

Three dimensional real-time ultrasound imaging has been a fact for over a decade now [1, 2]. It has not become a routine scanning modality because of poor resolution and contrast among other reasons. The major impediments are two - the prohibitively large number of channels, and the scan method.

The resolution of an image is determined by the size of the aperture. Conventional 2-D scanners use linear arrays with 64 to 128 active elements at a time. Extending the linear arrays to 3-D, would result in 4096 to 16384 channels. Sparse array matrices must be used in order to decrease the channel number [1, 3, 4].

Conventional B-mode scans contain roughly between 100 and 250 lines per image. The pulse repetition frequency is typically 5000 – 7000 Hz, which results in frame rates of up

to 50 frames per second. A real-time 3-D system must provide similar acquisition rates. Even if only 60 – 70 lines are beamformed in the azimuth and elevation directions, the volume will still contain up to 5000 lines. If they are scanned one-by-one, a volume will be acquired in about a second - too slow for dynamic visualization of the anatomy.

A solution to these problems can be provided by synthetic aperture (SA) imaging. A key feature of SA imaging is that the transmissions and the size of the acquired volume (number of lines) are decoupled.

Previous attempts to use synthetic transmit aperture imaging in combination with a mechanically rotating transducer proved successful [5]. Transducers with mechanical parts are generally considered less reliable than their fully electronic counterparts, so a natural next step is to investigate the use of multi-static SA imaging using a matrix array. The goal of this work is to investigate the possibility to implement 3D synthetic aperture imaging on the scanner RASMUS [6]. An overview of the system is given in Section II, in which the suggested implementation based on the system limitations is presented. The basic problem to be solved in SA *ultrasound* imaging of how to send more energy is discussed in Section III. The beamformation and the results from simulations are discussed in Sections IV and V.

II SYSTEM OVERVIEW

The purpose of the study is to investigate whether one can hope to acquire data for images with adequate quality using the experimental system RASMUS, developed by the Center for Fast Ultrasound Imaging.

The experimental system, on which the imaging will be implemented, has the ability to store raw 16-bit RF data from 64 receive channels for 3 seconds sampled at a sampling frequency of 40 MHz [6]. The system has 128 transmit and 64 receive digital channels. The 64 receive channels can be multiplexed to 128 transmit/receive amplifiers.

A decision was taken to use a 32×32 two dimensional array transducer such as the one offered by Vermon, Tours, France [7]. While the probe has a total of 1024 elements, the

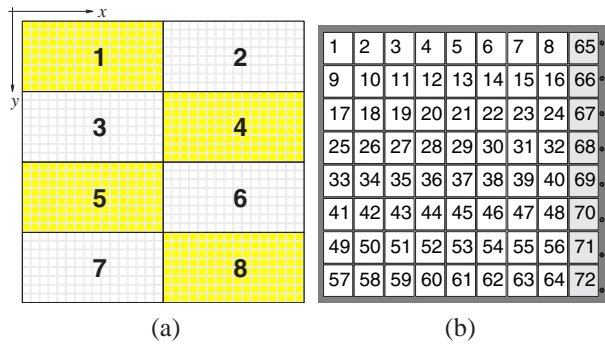


Figure 1: Numbering of the sub-apertures - (a), and numbering of elements in a sub-aperture - (b).

system has only 128 transceivers. A total of 128 8-to-1 multiplexors will connect the *analog* transmitters and receivers to the transducer elements. So each of the transmit digital channels will be connected to 8 elements of the transducer. The chosen multiplexors can change their position between every two emissions, but they are not fast enough to change position within a single pulse-echo event. Although all of the transducer elements will be routed to receivers and transmitters, only 128 of them will be accessed at a time, and these 128 elements will be the same for both transmit and receive. In order to increase the transmitted energy, one must transmit with a number of elements simultaneously. For linear arrays, the number is between 10 and 20. Similar penetration depth could be achieved with the matrix array, if one transmits with more than a 100 transmit elements every time since the area of the active aperture is the same.

Fig. 1 (a) shows how the transducer elements are divided into 8 sub-apertures of 128 elements each. Fig. 1 (b) gives the connections between the elements and the transducer elements in a single sub-aperture (block). Each block contains 16×8 elements. Inside a block the elements are divided into two sub-blocks of 8×8 elements each. The reason for this is that the 64 digital receive channels are already multiplexed to the analog front end. Digital channel # 1 can access analog channels #1 and #65, #2 can access #2 and #66, and so on. The shown configuration gives the possibility to select any compact block of 16×8 elements to transmit with, and within that block 64 elements can be routed to the receive channels. It is therefore possible to slide the whole aperture one element at a time in both the azimuth and elevation directions.

This configuration determines the scanning procedure - multi-static SA imaging, in which the source of the transmitted wave serves as the center of the receive aperture.

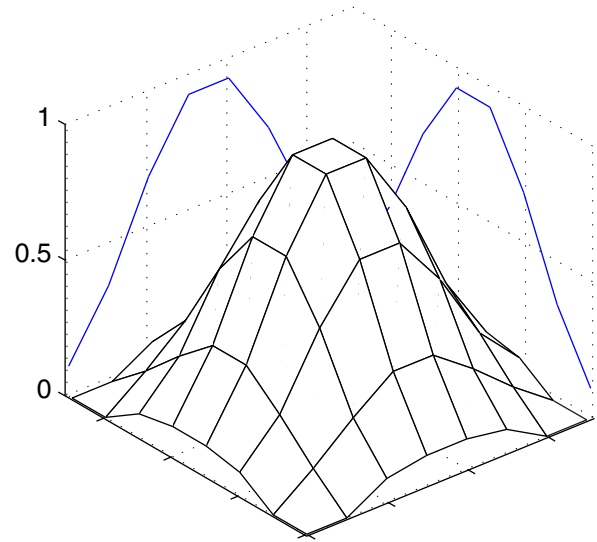


Figure 2: The transmit apodization

III THE TRANSMISSION

For 3-D SA imaging a spherical wave must be transmitted to collect information from the whole region under investigation. Such a wave can be created in three ways: (a) transmit with a single element, (b) transmit a *de*-focused wave with a sub-aperture, and (c) transmit a focused wave, where the focus is set very close to the transducer surface. Transmitting with a single element gives the largest flexibility in selecting transducer elements for receive, but the transmitted energy is too low to be used for imaging. The use of *de*-focused transmits has so far been the most common way of generating spherical waves [5, 8, 9]. A spherical wave can be approximated by transmitting with the central element first and with the outermost elements last. The equation for the delays is:

$$r = \max(N_{ax}, N_{ay}) \cdot d_x \quad (1)$$

$$\tau_i = \frac{1}{c} \left(\sqrt{x_i^2 + y_i^2 + r^2} - r \right), \quad (2)$$

where the coordinates of the element i x_i and y_i are given relative to the center of the active subaperture. N_{ax} and N_{ay} are the number of elements in the x and y directions, respectively.

One of the problems, when trying to create a spherical wave using multiple elements, is the presence of edge waves due to diffraction. The effect of the edge waves is exhibited in the appearance of a second peak in the axial direction. The amplitude of this peak may reach -30 dB from the peak value. The edge waves are reduced by setting apodization in transmit. It was determined that the footprint of the apodization should not be rectangular, but elliptical or circular. Several windowing functions were considered, and the following was

Center frequency	f_0	2.93 MHz
Speed of Sound	c	1540 m/s
Wavelength	λ	0.526 mm
Element pitch	d_x, d_y	0.3 mm $\approx 0.6\lambda$
Element size	$w_x \times w_y$	0.27×0.27 mm
Number of elements	$N_x \times N_y$	32×32
Active elements	$N_{a_x} \times N_{a_y}$	8×8

Table 1: Simulation parameters

experimentally found to give the lowest amplitude of the edge waves:

$$R_x = \frac{N_{a_x} d_x}{2} \quad (3)$$

$$R_y = \frac{N_{a_y} d_y}{2} \quad (4)$$

$$b_i = \frac{x_i^2}{R_x^2} + \frac{y_i^2}{R_y^2} \quad (5)$$

$$a_i = 0.54 - 0.46 \cdot \cos(\pi(1 - \sqrt{b_i})) \quad (6)$$

An 8×8 aperture was used in transmit and the footprint was set to be circular.

IV THE BEAMFORMATION

The image is created using a standard delay-and-sum beamforming:

$$\mathbf{H}(\vec{x}) = \sum_{i \in \Omega_{xmt}} \sum_{j=1}^{N_r} a_{ij}(\vec{x}) r_{ij}(t_{ij}(\vec{x})) \quad (7)$$

$$t_{ij}(\vec{x}) = \frac{1}{c} (|\vec{x} - \vec{x}_i| + |\vec{x} - \vec{x}_j|), \quad (8)$$

where $r_{ij}(t)$ is the signal received by the j th element after transmitting with the i th *virtual* element, $a_{ij}(\vec{x})$ are the weighting coefficients, and Ω_{xmt} is the set of transmitting *virtual* elements. The spatial position, which the origin of the transmitted wavefront can be traced to, is considered to be a virtual element. For practical reasons, the center of the active transmit sub-aperture is chosen as the virtual source. If the number of elements in active sub-aperture is large (> 10 in one direction), then the introduced phase error must be compensated for.

V SIMULATION RESULTS

The simulations were done in Field II [10, 11]. The simulation parameters are listed in Table 1. They have been set to match the production parameters of the 2-D array made by Vermon [7], which is the target array for the implementation. To obtain good results in

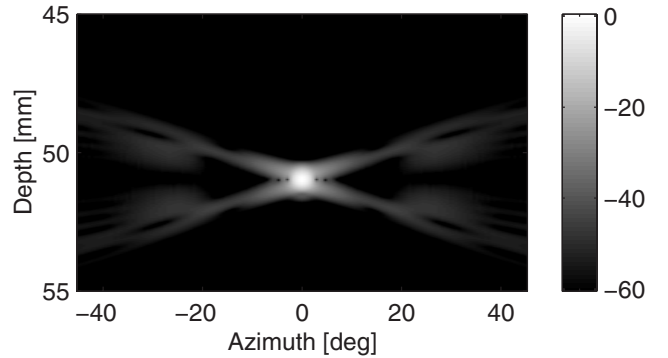
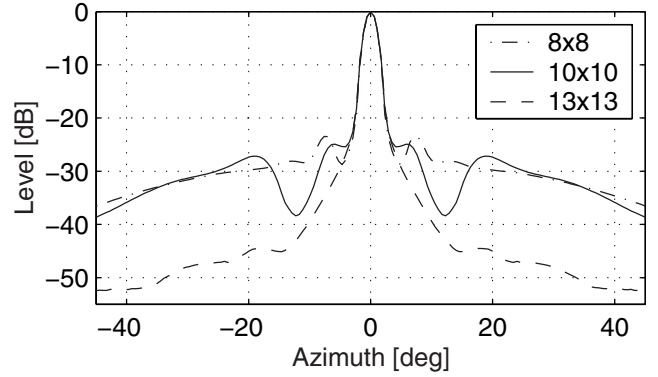
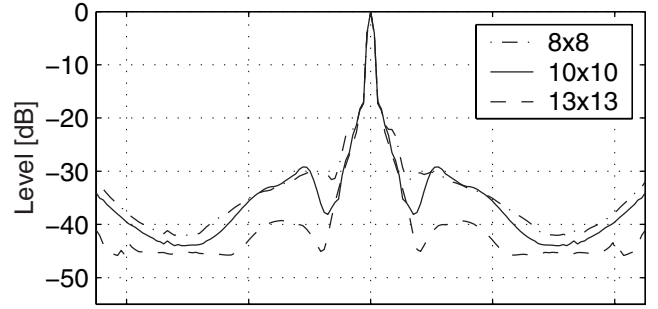


Figure 3: Cross section of the point spread function in the azimuth plane. Three cases are shown in each of the plots - for 64, 100, and 169 transmissions. The number of transmit centers along the azimuth and elevation directions is the same: 8 by 8, 10 by 10, or 13 by 13, respectively. The top plot is made using boxcar apodization in receive. The middle plot is made using Hamming apodization in receive. The bottom image is a B-mode cross section when 13×13 emissions were used.

Field II, the simulation was performed at a sampling frequency of 120 MHz. The resulting signal was down-sampled to 40 MHz and 16 bit precision. The beamformation was done using linear interpolation (A Matlab toolbox is available at: <http://www.oersted.dtu.dk/~personal/sn/ultrasound.imaging/?BFT/>)

A sub-aperture of 8×8 elements was used to transmit and receive with. Two cases were simulated - with rectangular receive apodization and with hamming receive apodization. The transmissions were uniformly distributed over the transducer elements, and the point spread functions are symmetric in both azimuth and elevation direction.

Figure 3 shows the result of using a different number of transmit events. The top plot shows the case when a rectangular window was used as a receive apodization, and the middle plot when the receive apodization was circularly symmetric hamming window. The bottom sub-figure is a B-mode cross-section for the case of 169 (13×13) emissions. On each of the plots three cases are shown, for 64, 100, and 169 transmissions. If the pulse repetition frequency is 5000 Hz, then this translates in frame rates of 70, 50 and 30 frames / second, which satisfies the real-time needs for an ultrasound system. In-vivo synthetic aperture ultrasound has been previously implemented using a similar number of emissions, but for the 2-D case [12].

The general trend is as expected - more transmit events result in lower the side lobes. For the case of using hamming windowing in receive, the peak grating-lobe level is -23.5 , -25 , -44.5 dB below the main peak for 64, 100, and 169 transmit events, respectively.

The bottom image in Fig. 3 shows that the apodization used in transmit successfully suppresses the edge waves, and that there are no secondary peaks in the azimuth direction. The point-spread-function is symmetric, confirming that the phase error associated with the use of multiple elements is negligible for the 8×8 sub-aperture used in the imaging procedure.

VI CONCLUSION

This paper presented the first step towards the implementation of a real-time 3-D synthetic aperture imaging system. It has been shown that useful 3-D images could be obtained using between 100 and 200 transmissions, and careful selection of the imaging parameters, such as delay calculations and weighting coefficients.

The investigation did not include noise, frequency dependent attenuation and motion artifacts. However, a similar number of emissions has previously successfully used to create *in-vivo* SA images.

Only one pattern of transmissions was presented. It uses only 64 of the available 128 channels at a time, which gives the possibility of selecting some other element patterns to reduce further the side-lobe energy.

VII ACKNOWLEDGMENTS

This work was supported by grant 9700883, 9700563 and 26-01-0178 from the Danish Science Foundation and by B-K Medical A/S Denmark.

VIII REFERENCES

- [1] S. W. Smith, H. G. Pavy, and O. T. von Ramm. High-speed ultrasound volumetric imaging system – Part I: Transducer design and beam steering. *IEEE Trans. Ultrason., Ferroelec., Freq. Contr.*, 38:100–108, 1991.
- [2] O. T. von Ramm, S. W. Smith, and Henry G. Pavy. High-speed ultrasound volumetric imaging system – Part II: Parallel processing and image display. *IEEE Trans. Ultrason., Ferroelec., Freq. Contr.*, 38:109–115, 1991.
- [3] G. R. Lockwood and F.S. Foster. Design of sparse array imaging systems. In *Proc. IEEE Ultrason. Symp.*, pages 1237–1243, 1995.
- [4] S. I. Nikolov and J. A. Jensen. Application of different spatial sampling patterns for sparse array transducer design. *Ultrasonics*, 37(10):667–671, 2000.
- [5] S. I. Nikolov, R. Dufait, A. Schoisswohl, and J. A. Jensen. Three-dimensional real-time synthetic aperture imaging using a rotating phased array transducer. In *Proc. IEEE Ultrason. Symp.*, pages 1545–1548, 2002.
- [6] J. A. Jensen, O. Holm, L. J. Jensen, H. Bendsen, H. M. Pedersen, K. Salomonsen, J. Hansen, and S. Nikolov. Experimental ultrasound system for real-time synthetic imaging. In *Proc. IEEE Ultrason. Symp.*, volume 2, pages 1595–1599, 1999.
- [7] L. Ratsimandresy, P. Mauchamp, D. Dinet, N. Felix, and R. Dufait. A 3 MHz two dimensional array based on piezocomposite for medical imaging. In *Proc. IEEE Ultrason. Symp.*, pages 1265–1268, 2002.
- [8] M. Karaman, P. C. Li, and M. O’Donnell. Synthetic aperture imaging for small scale systems. *IEEE Trans. Ultrason., Ferroelec., Freq. Contr.*, 42:429–442, 1995.
- [9] G. R. Lockwood, J. R. Talman, and S. S. Brunke. Real-time 3-D ultrasound imaging using sparse synthetic aperture beamforming. *IEEE Trans. Ultrason., Ferroelec., Freq. Contr.*, 45:980–988, 1998.
- [10] J. A. Jensen and N. B. Svendsen. Calculation of pressure fields from arbitrarily shaped, apodized, and excited ultrasound transducers. *IEEE Trans. Ultrason., Ferroelec., Freq. Contr.*, 39:262–267, 1992.
- [11] J. A. Jensen. Field: A program for simulating ultrasound systems. *Med. Biol. Eng. Comp.*, 10th Nordic-Baltic Conference on Biomedical Imaging, Vol. 4, Supplement 1, Part 1:351–353, 1996b.
- [12] K. L. Gammelmark and J. A. Jensen. Multielement synthetic transmit aperture imaging using temporal encoding. *IEEE Trans. Med. Imag.*, 22(4):552–563, 2003.